EuroIntervention 2022;18:83-90 published online ahead of print December 2021

Bench test and in vivo evaluation of longitudinal stent deformation during proximal optimisation

Gabor G. Toth[1]*, MD, PhD; Alexandru Achim[1,2], MD; Marcel Kafka[1], MD; Xinlei Wu[3], MD, PhD; Mattia Lunardi[3], MD; Sinjini Biswas[4], MD; Atif Shahzad[3,5], MD, PhD; Attila Thury[2], MD, PhD; Zoltan Ruzsa[2], MD, PhD; Thomas W. Johnson[4], MD, PhD; William Wijns[3], MD, PhD

1. University Heart Center Graz, Department of Cardiology, Medical University of Graz, Graz, Austria; 2. Second Department of Internal Medicine, Division of Invasive Cardiology, University of Szeged, Szeged, Hungary; 3. The Lambe Institute for Translational Medicine, Smart Sensors Lab and Curam, Saolta University Healthcare Group, Galway, Ireland; 4. Bristol Heart Institute, University of Bristol, Bristol, United Kingdom; 5. Centre for Systems Modelling and Quantitative Biomedicine, University of Birmingham, Birmingham, United Kingdom

This paper also includes supplementary data published online at: https://eurointervention.pcronline.com/doi/10.4244/EIJ-D-21-00824

KEYWORDS

- bifurcation
- drug-eluting stent
- left main

Abstract

Background: While radial stent deformation has been thoroughly investigated, data on longitudinal deformation are scarce.

Aims: The aim of the study was to describe longitudinal stent deformation associated with the proximal optimisation technique (POT).

Methods: Longitudinal stent deformation was assessed by bench testing and by clinical evaluation. Bench testing was performed in silicone models using 3.00 (n=15) and 3.50 mm (n=14) stent platforms. After deployment, stents were sequentially post-dilated in the proximal main branch up to 5.50 mm, in increments of 0.50 mm, in order to simulate a spectrum of overexpansion. Stent length was redefined by optical coherence tomography (OCT) after each step. Clinical data were collected retrospectively from OCT-guided bifurcation percutaneous coronary intervention cases.

Results: In bench tests, POT has led to significant stent elongation in all cases. The magnitude of elongation was comparable between the 3.00 and the 3.50 mm stent platforms, with 0.86±0.74 mm vs 0.86±0.73 mm, respectively (p=0.71), per 0.5 mm overexpansion. For 3.00 mm stent platforms, maximal elongation was 4.31±1.47 mm after up to 5.5 mm overexpansion. For 3.50 mm platforms, maximal elongation was 2.87±0.94 mm after up to 5.5 mm overexpansion. Thirty-six clinical cases were analysed, of which 22 (61%) were performed in the distal left main. Post-dilation was performed with 0.98±0.36 mm absolute overexpansion, resulting in 2.22±1.35 mm elongation, as compared to nominal stent length.

Conclusions: Overexpansion by POT results in proximal stent elongation. This has to be considered once the stent length is selected and the stent is positioned, especially in the left main stem, where proximal overexpansion is marked and accurate ostial landing is critical.

**Corresponding author: University Heart Center Graz, Department of Cardiology, Medical University of Graz, Auenbruggerplatz 15, 8036 Graz, Austria. E-mail: gabor.g.toth@medunigraz.at*

SUBMITTED ON 17/09/2021 - REVISION RECEIVED ON 01/11/2021 - ACCEPTED ON 15/11/2021

DOI: 10.4244/EIJ-D-21-00824

Abbreviations

dMB	distal main branch
OCT	optical coherence tomography
PCI	percutaneous coronary intervention
pMB	proximal main branch
POT	proximal optimisation technique

Introduction

The fractal geometry of coronary bifurcations defines a relevant diameter mismatch between the proximal main branch (pMB) and daughter branches. Accordingly, the treatment of bifurcation lesions poses technical challenges for the current stent platforms which are designed with tubular geometry.

Percutaneous coronary intervention (PCI) of bifurcation lesions can be performed using various techniques, depending on the plaque distribution across the main and daughter branches, and the bifurcation geometry[1]. Regardless of the selected stenting technique, one common step is shared, namely the proximal optimisation technique (POT)[2]. Briefly, the stent is sized according to the distal main branch (dMB) reference diameter in order to avoid distal vessel trauma and excessive carina shifting. As a result, stent deployment is undersized according to the pMB reference diameter[3,4]. The resulting proximal undersizing and strut malapposition have to be corrected by proper post-dilation of the proximal stent segment from its proximal edge to the level of the carina, using a balloon sized according to the reference diameter of the pMB.

Depending on the magnitude of diameter mismatch, a proper POT can expose the stent to extreme overexpansion, resulting in relevant structural deformation. While expansion capacities and radial deformation have been thoroughly investigated[5,6], less data are available on "longitudinal behaviour". Still, its clinical relevance is major, particularly in the case of left main stem, where the calibre discrepancy is greatest and accurate aorto-ostial landing is crucial. Accordingly, our study aims to analyse and describe the longitudinal deformation pattern of stents during overexpansion with POT.

Methods

BENCH TESTING

SILICONE BENCH MODEL

POT was simulated in two different models. Both models had a proximal segment (representing the proximal main branch [pMB]) of >6.00 mm inner lumen diameter. A short transition zone of 1.00 mm length connected the proximal segment with a distal segment (representing the distal main branch [dMB]) with an inner lumen diameter sized according to the nominal size (i.e., 3.00 or 3.50 mm) of the stents used for bench testing **(Supplementary Figure 1)**. This model allows the simulation of resistance-free stent opening in a wide spectrum of different diameter mismatch scenarios between the proximal main and distal daughter branches. The bench model was made of rubber-like elastomeric material, Köraform A 42 RTV silicon (CHT).

PROCEDURE

Stent deformation during POT was tested for the 3.00 and 3.50 mm stent platforms in five different designs: Orsiro (Biotronik AG), Resolute Onyx (Medtronic), SYNERGY (3.0 mm) and SYNERGY MEGATRON (3.5 mm) (both Boston Scientific), Ultimaster (Terumo) and XIENCE (Abbott). All stents were ≥28 mm long. Considering that in practice, the stent length in pMB can also vary, each stent type was tested for optimisation on proximal segments 10, 15 and 20 mm long.

Stents were first deployed with nominal pressure, having the predefined POT segment length protruding into the pMB. This was followed by POT in multiple steps of incremental diameters of 0.50 mm up to 5.50 mm, in order to simulate and describe the wide spectrum of overexpansion within the on-label range and beyond **(Supplementary Figure 2)**. Only non-compliant balloons were used for the POT, always at nominal pressure. The POT balloon was positioned with its distal marker, accurately located at the proximal end of the transition zone, simulating the level of the carina. Importantly, balloons were always completely deflated first and removed under visual control in order to avoid any stent entrapment when pulling back the deflated balloon catheter. It is important to note that the very large calibre of the pMB (i.e., >6 mm) was purposely chosen to allow stent expansion without any extrinsic resistance.

OPTICAL COHERENCE TOMOGRAPHY (OCT)

OCT imaging was undertaken systematically twice after stent implantation and following every POT step for the assessment of stent length in the pMB, stent length in the dMB and total stent length. Before OCT pullback imaging, the guidewire was removed to avoid shadow artefact. A Dragonfly Duo (Abbott) OCT catheter was used and images were analysed by a dedicated workstation (C7-XR OCT Intravascular Imaging System; Abbott). Images were recorded at 100 frames per second. Each pullback was analysed by two blinded investigators (A. Achim and M. Kafka) independently, unaware of stent type, stent size, or post-dilatation step.

CLINICAL ASSESSMENT

The OCT databases of the four participating centres (University Heart Center Graz; University of Szeged; Saolta University; Bristol Heart Institute) were screened for two years, retrospectively, to identify cases, fulfilling the following criteria: (1) bifurcation PCI with POT performed, with or without kissing dilation; (2) final OCT available with sufficient image quality; (3) the entire stent length is included in one OCT pullback; and (4) no overlapping stents present.

Based on OCT images, the stent length in the pMB, the stent length in the dMB and the total stent length were measured. According to procedural reports, the nominal size of the POT balloon was taken as POT diameter and it was not adapted to pressure-diameter charts. Analysis of OCT recordings was conducted in the context of a clinical registry of OCT-guided bifurcation PCI cases, approved by the Ethics Committee of the University of Szeged.

STATISTICAL ANALYSIS

All analyses were performed with Prism GraphPad 5.0 (GraphPad Software Inc.). Summary descriptive statistics are reported as mean±SD. Stent lengths after different steps were compared by ANOVA with Greenhouse-Geisser correction and by paired t-test before and after each step. Stent lengths for different models and for different POT segments were compared by ordinary ANOVA and by unpaired t-test before and after each step. For the bench procedures, each step was imaged by OCT twice and two independent investigators analysed each pullback image. For the analysis, the average of these four calculations was taken. For the clinical cases, one single final OCT pullback image was considered. A probability value of $p<0.05$ was considered as significant.

Results

BENCH SIMULATION

In total, 15 test procedures were performed with the 3.0 mm stent platforms (three of each stent brand) and 14 test procedures were performed with the 3.5 mm stent platforms (three of each stent brand, except SYNERGY MEGATRON with two tests). For the 3.0 mm platform, as compared to the nominal stent length, significant lengthening was observed after each 0.5 mm incremental POT step. This was due to significant elongation in the pMB, while no relevant change was observed in the dMB **(Figure 1A, Figure 2, Table 1)**. A maximal elongation length of 4.31±1.47 mm was observed in the pMB following 5.5 mm overexpansion, reaching 27.77±7.90% relative elongation, without significant change in the dMB (0.09±0.44 mm). The same effect was observed for the 3.5 mm platform with significant lengthening after each 0.5 mm incremental overexpansion step, except following the 4.0 mm post-dilation **(Figure 1B, Figure 2, Table 1)**. Here the maximal elongation after 5.5 mm overexpansion was 2.87±0.94 mm in the pMB, reaching 19.45±6.37% relative elongation. Deformation in the dMB was 0.28±0.19 mm. Elongation per step of 0.5 mm post-dilation was comparable between the 3.00 mm and the 3.50 mm stent platforms (0.86±0.74 mm vs 0.86±0.73 mm,

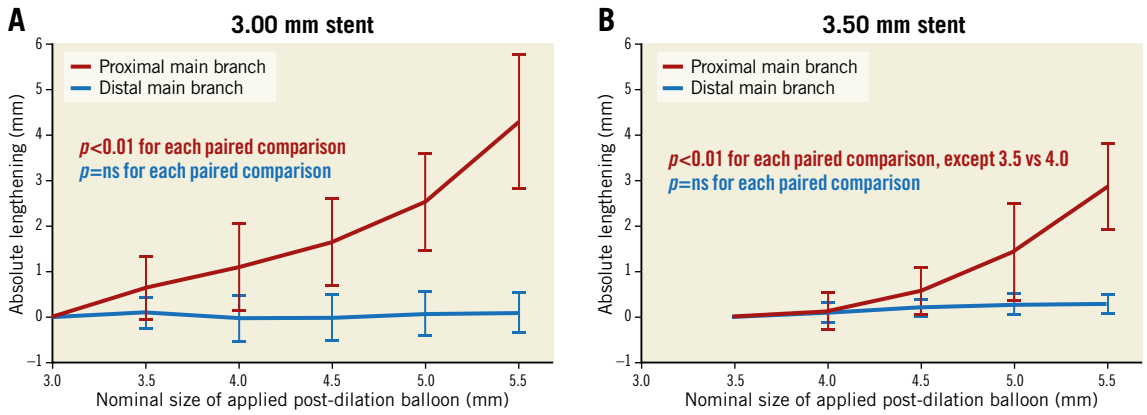

Figure 1. *Longitudinal stent behaviour during proximal optimisation in 3.00 mm stent platforms (A) and in 3.50 mm stent platforms (B) in bench.*

Table 1. Absolute and relative longitudinal stent deformation in the proximal main branch and the distal main branch during proximal optimisation in bench.

3.00 mm platform n=15						
POT	Δlength in pMB	Δ%	*p*-value*	Δlength in dMB	Δ%	*p*-value*
3.00 mm	reference value	–	–	reference value	–	–
3.50 mm	+0.63±0.69 mm	+3.6±3.7%	<0.01	+0.09±0.33 mm	+0.5±2.3%	0.18
4.00 mm	+1.10±0.96 mm	+7.3±6.8%	<0.01	–0.03±0.51 mm	–0.4±3.5%	0.81
4.50 mm	+1.65±0.96 mm	+10.8±6.6%	<0.01	–0.02±0.51 mm	–0.4±3.6%	0.21
5.00 mm	+2.53±1.07 mm	+16.4±5.6%	<0.01	+0.06±0.49 mm	+0.4±3.4%	0.61
5.50 mm	+4.31±1.47 mm	+27.8±7.9%	<0.01	+0.10±0.44 mm	+0.4±3.1%	0.31
3.50 mm platform n=14						
POT	Δlength in pMB	Δ%	*p*-value*	Δlength in dMB	Δ%	*p*-value*
3.50 mm	reference value	–	–	reference value	–	–
4.00 mm	+0.12±0.40 mm	+0.8±3.1%	0.28	+0.10±0.22 mm	+0.5±1.8%	0.12
4.50 mm	+0.56±0.52 mm	+3.8±3.9%	<0.01	+0.20±0.17 mm	+1.3±1.2%	0.12
5.00 mm	+1.43±1.07 mm	+9.8±8.9%	<0.01	+0.28±0.24 mm	+2.2±1.7%	0.11
5.50 mm	+2.87±0.94 mm	+19.5±6.5%	<0.01	+0.28±0.19 mm	+2.3±1.6%	0.23

**p*-value relates to the comparison with the previous step. dMB: distal main branch; pMB: proximal main branch; POT: proximal optimisation technique

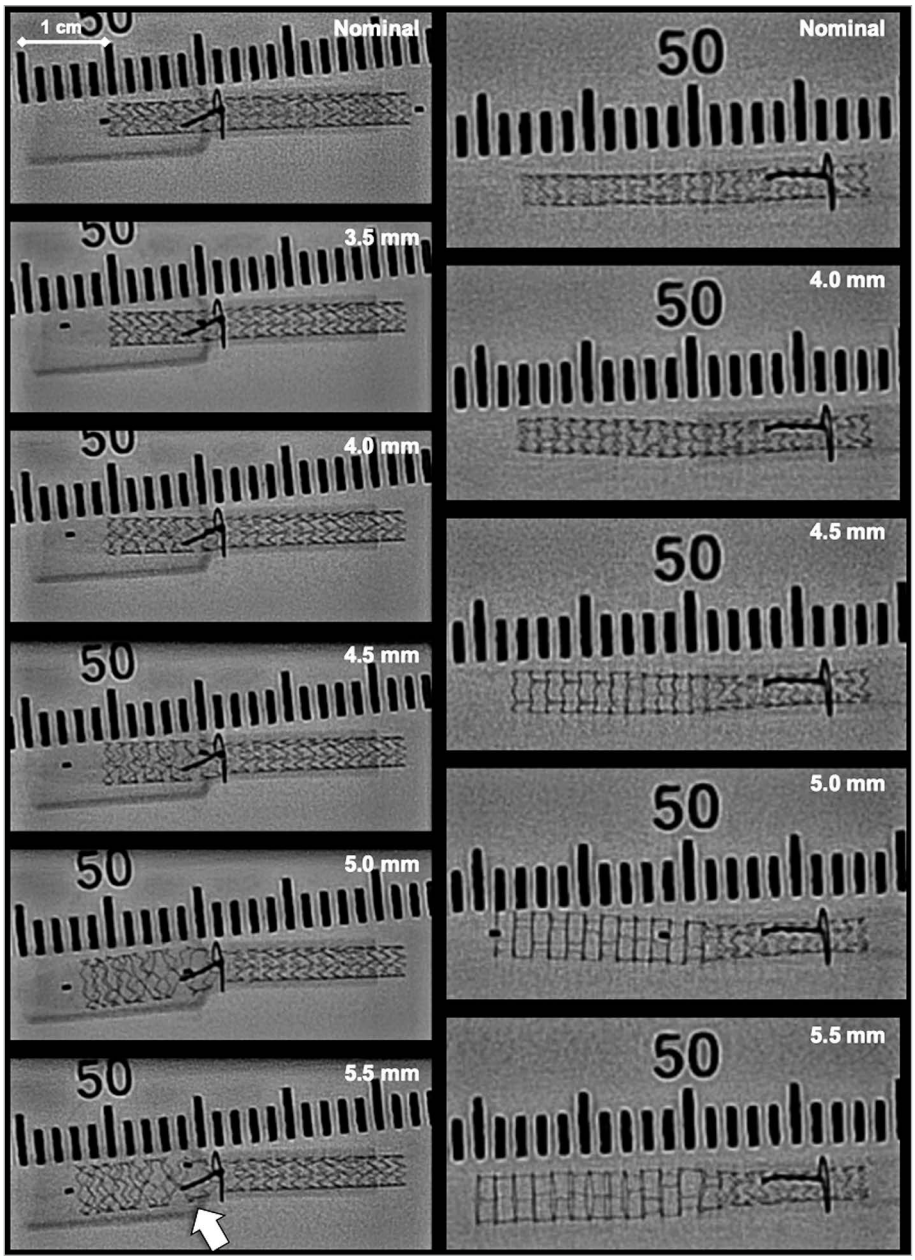

Figure 2. *Bench observation of lengthening in 3.00 mm stent platforms (left column) and in 3.50 mm stent platforms (right column). Ruler scale is per two millimetres. White arrow indicates the stretching of the strut construction at the level of the distal branch ostium.*

respectively; p=0.71) **(Figure 3A)**. The magnitude of elongation between two post-dilations increased with the number of steps from 0.69±0.58 mm to 1.75±0.70 mm (p<0.01) for the 3.00 mm platform and from 0.21±0.53 mm to 1.65±0.66 mm (p<0.01) for the 3.50 mm platform **(Figure 3B, Figure 3C)**. A significant difference has been found when comparing the overall elongation tendency for 10 mm vs 15 mm vs 20 mm pMB segments (1.34±1.36 mm vs 1.64±1.30 mm vs 2.12±1.89 mm, respectively; p=0.05). No significant difference was found either by comparing different stent types or by comparing 2- versus 3-connector designs **(Supplementary Figure 3A, Supplementary Figure 3B)**. OCT analysis did not show any strut fracture.

CLINICAL ASSESSMENT

In total 36 eligible cases were identified and analysed, of which 22 (61%) cases were performed in the distal LM bifurcation, 13 (36%) in the left anterior descending artery and diagonal bifurcation and one case in the crux of the right coronary artery. Nominal stent diameter was 3.31±0.34 mm and nominal length was 26.14±9.03 mm. Proximal optimisation was performed with 0.98±0.36 mm absolute overexpansion, which equals 30.29%±12.98% relative overexpansion. The final OCT images demonstrated 2.22±1.35 mm elongation on average as compared to the nominal stent length (p<0.01) **(Central illustration, Figure 4, Supplementary Table 1)**. No statistical difference was found when

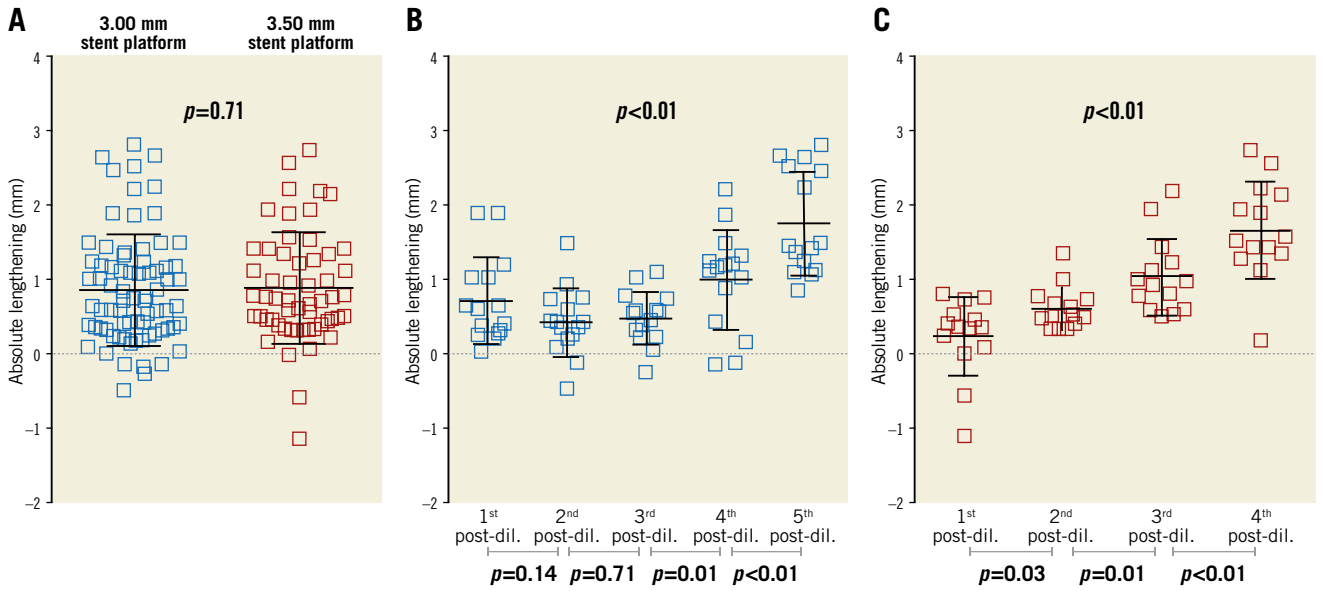

Figure 3. *Comparison of absolute lengthening. A) Overall in 3.00 mm (blue) and 3.50 mm (red) stent platforms and per steps of overdilation (B) for 3.00 mm and (C) for 3.50 mm platforms.*

elongation was assessed according to the tertiles of overexpansion **(Supplementary Table 1, Supplementary Figure 4)**.

Discussion

Our study, utilising bench modelling and the analysis of clinical cases with OCT-guided bifurcation PCI, provides novel insights into the stent deformation, related to POT. We report that bench-simulated POT leads to relevant elongation of the implanted stent at the level of the pMB. Slight elongation can be observed even after 0.5 mm overexpansion, however this can extend to more than 4 mm in case of off-label overexpansion. Retrospective analysis of OCT-guided bifurcation PCI cases replicates this finding with, on average, greater than 2 mm stent elongation in the pMB stent segment. These observations are at variance with the commonly accepted belief that POT mostly results in stent shortening.

Significant malapposition and underexpansion are responsible for poor post-PCI functional results and are associated with target lesion failure and stent thrombosis, therefore they have to be corrected[7-9]. POT, which is considered to be mandatory by the latest expert consensus document, facilitates stent apposition in the pMB, optimises strut clearance across the jailed side branch ostium and corrects instrumentation-related stent deformation[1]. Excessive overexpansion of the stent, commonly needed during left main PCI[10] due to a pronounced calibre discrepancy between the pMB and distal branches, combined with interaction between the post-dilatation balloon, stent and bifurcation geometry, may result in longitudinal stent deformation. While radial deformation has been thoroughly investigated and described in detail by manufacturers and clinical investigators[5,6], much less is known about the longitudinal deformation of stents. The first clinical series of longitudinal stent deformation, reported by Williams at al, focused on the mechanical disruption secondary to device

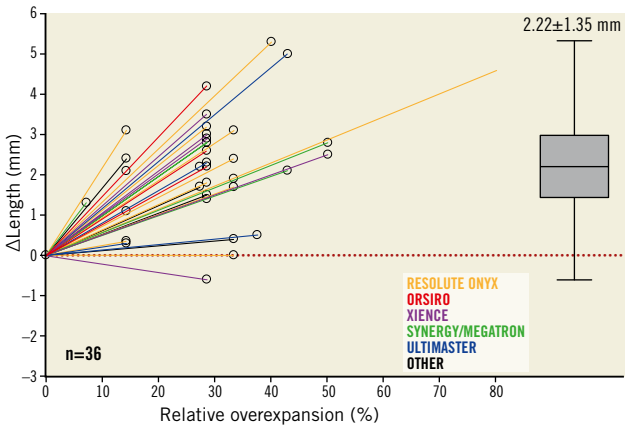

Central illustration. *Observed longitudinal stent deformation in clinical cases per case (left) and overall (right). Dotted red line indicates reference.*

passage through deployed stents[11]. The same observation was analysed in depth by Ormiston et al[12,13] providing detailed analysis of longitudinal stent deformation patterns, mostly due to extrinsic compression. Conversely, the propensity for intrinsic elongation was investigated in a previous bench study using a tapered vessel model, showing that stents tended to lengthen by up to 2 mm after 0.25 to 0.50 mm oversized focal proximal post-dilation[14]. Matsuda et al showed that a malapposed stent arc of more than 180 degrees is predictive for significant elongation. This observation suggests that a malapposed stent segment (as represented by our model) can expand freely in the axial dimension. While in the case of apposed but undersized stents (i.e., like in case of a Medina 1,x,x stenosis) less elongation is expected once post-dilated[15].

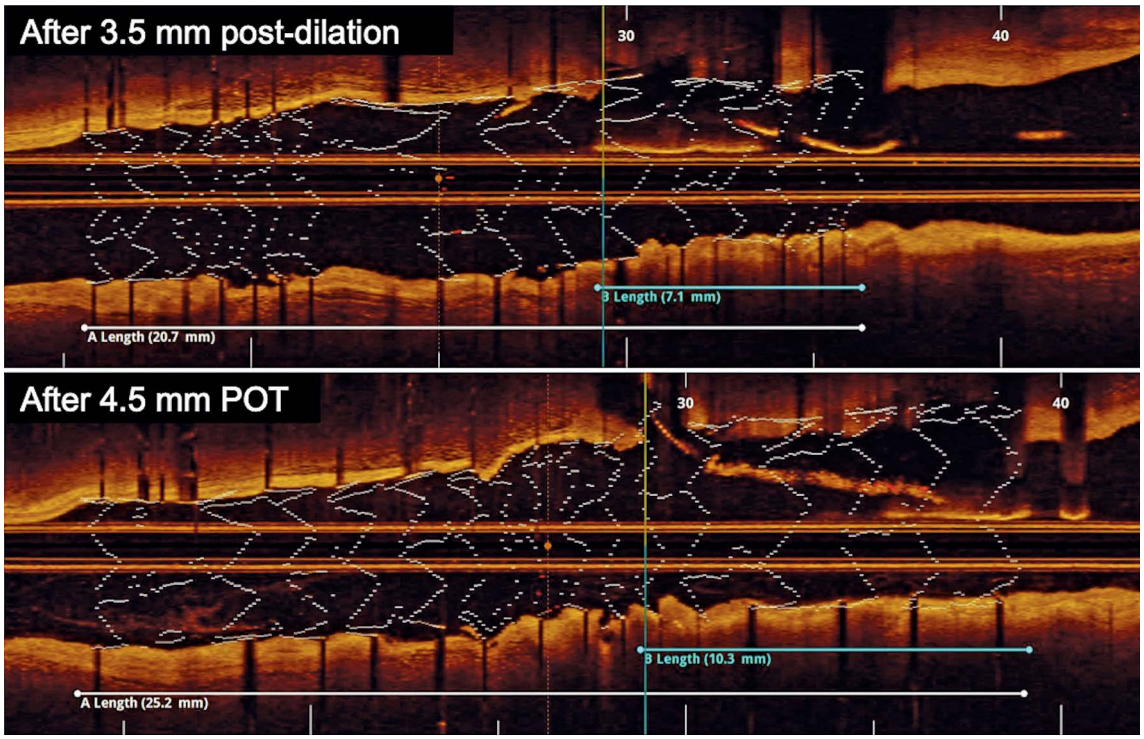

Figure 4. *Case example. Lengthening of the proximal portion of a 3.0 mm stent after 4.5 mm proximal optimisation as shown by optical coherence tomography. POT: proximal optimisation technique*

The present study is the first to analyse overexpansion-related longitudinal deformation in a systematic and detailed manner, facilitating a better understanding of the mechanisms and the magnitude of stent elongation after POT. These findings are of utmost importance for optimising current practices, especially for left main stem interventions where overdilation can be massive and accurate ostial landing is crucial.

From our findings we have identified two different mechanisms behind elongation: (1) the overexpansion with tight 'balloon-to-strut' interaction results in stretching of crowns and connectors longitudinally; (2) the "correctly positioned" POT balloon slides backwards during opening, pulling stent struts back from the dMB ostium **(Moving image 1, Moving image 2)**. The latter is related to POT balloon characteristics. When the balloon is positioned with the radio-opaque marker at the level of the carina, its conical tip protrudes into the dMB and still relatively oversized its lumen. It therefore tends to slip backwards during inflation ("melon seed effect"; **Figure 5A1-Figure 5A3**), resulting in axial stent stretching and disruption of the stent architecture at the daughter vessel ostium **(Figure 2)**. The latter might be associated with suboptimal scaffolding by reduction of metal-to-vessel and drug-to-vessel ratios, a potential source of long-term device failure[16]. Further investigation was beyond the scope of the present study, still one can assume that the "melon seed effect" depends on the diameter mismatch, the design of the POT balloon **(Figure 5B)**, as well as the expansion resistance of the dMB ostium (i.e., amount of calcium or fibrosis).

During left main intervention, the observed stent elongation can result in clinically relevant pitfalls. Failing to recognise this phenomenon may lead to dynamic protrusion into the aorta, which has potential side effects such as strut damage induced by the guiding catheter, potential nidus for thrombus formation, plus difficulties with ostial catheter engagement and wire advancement upon secondary catheterisation. Accordingly, our findings have important clinical implications. First, rather than aiming for a perfect marker-on-carina position of the POT balloon, a modified (somewhat more proximal) position should be considered, adapted to the diameter mismatch and conus length of the available balloon. Second, instead of aiming for a perfect aorto-ostial position of the stent, potential proximal elongation should be accounted for, with positioning of the stent slightly within the ostium of the left main stem.

Limitations

The study has some limitations to be considered; first, a common limitation of bench models is that they fail to truly simulate the geometry and elasticity of diseased coronary vessels. Stent deployment in *de novo* coronary disease with differential distribution of fibrosis and calcification may behave differently to silicon. However, the clinical cases included in our present work are entirely confirmatory of the on-bench findings. Second, our findings pertain to a limited series of cases and only to the five tested stent platforms, while other designs might behave differently. However, almost all the latest generation stent platforms have conceptually similar open-cell designs and therefore deformation is expected to be similar. Third, the post-dilations went beyond

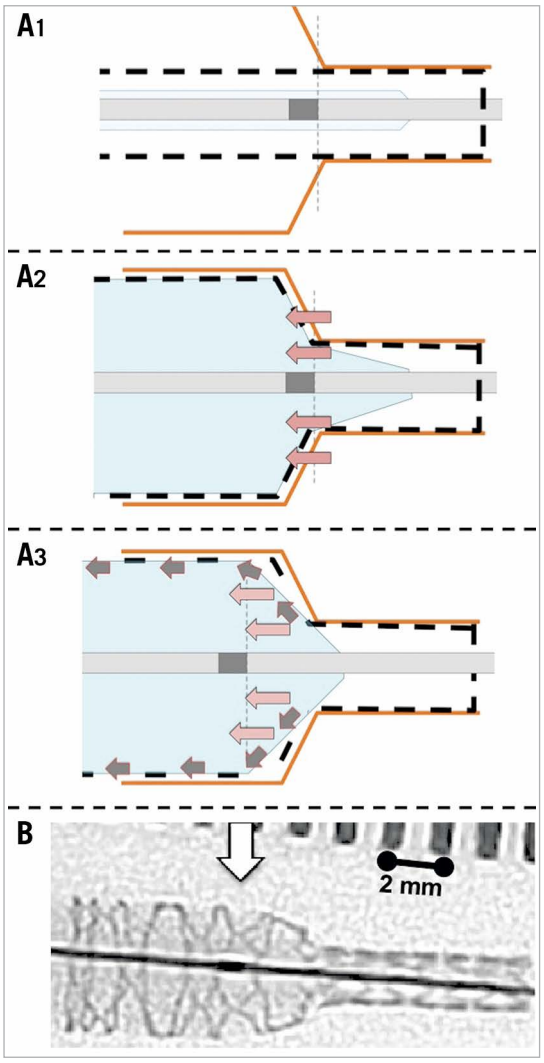

Figure 5. *The "melon seed effect" and design of the POT balloon. Mechanism of the "melon seed effect" of the POT balloon (A1-A3) and demonstration of the conical tip of a balloon catheter as compared to balloon marker (white arrow) (B). Red arrows indicate the proximal migration of the distal balloon edge. Grey arrows indicate the resulting separation of the stent struts at the level of the junction between pMB and dMB (corresponding to the carina in vivo). dMB: distal main branch; pMB: proximal main branch; POT: proximal optimisation technique*

the on-label capacities of the stents, suggested by manufacturers. Still, we believe that in daily clinical practice such manoeuvres are often needed and performed to avoid malapposition in large-sized proximal main branches. The impact of kissing dilation was also not tested in the present experiments. Similarly, the small sample size of clinical cases does not allow analysing the impact of kissing dilation. Fourth, for the *in vivo* cases, only the final OCT recordings were uniformly available.

Conclusions

Proximal optimisation technique in bifurcation PCI results in significant elongation of the proximal stent segment. Awareness of this phenomenon is important in everyday clinical practice, especially during left main PCI, and should be considered when selecting the stent length and during stent positioning.

Impact on daily practice

Contrary to common opinion, the proximal optimisation technique in bifurcation PCI results in significant elongation, rather than shortening, of the proximal stent segment. Accordingly, potential proximal elongation should be accounted for when selecting stent size and length, as well as during stent positioning. This has most relevance in case of left main PCI, where the overexpansion is massive and ostial landing for the stent is critical.

Acknowledgements

Testing equipment, including guidewires, stents and balloon catheters were provided by Abbott Laboratories Inc., Medtronic, Biotronik AG, Boston Scientific and Terumo Inc. without financial involvement or intellectual restriction.

Conflict of interest statement

G. Toth receives personal fees from Abbott, Medtronic, Terumo and Biotronik, outside the present work. T. Johnson has received personal fees from Abbott, Boston Scientific, Medtronic and Terumo, outside the present work. W. Wijns has received institutional research grants from MicroPort and is supported by a Science Foundation Ireland Research Professorship grant (15/RP/2765). X. Wu, M. Lunardi and A. Shahzad are supported by a Science Foundation Ireland Research Professorship grant (15/RP/2765). The other authors have no conflicts of interest to declare.

References

1. Burzotta F, Lassen JF, Lefèvre T, Banning AP, Chatzizisis YS, Johnson TW, Ferenc M, Rathore S, Albiero R, Pan M, Darremont O, Hildick-Smith D, Chieffo A, Zimarino M, Louvard Y, Stankovic G. Percutaneous coronary intervention for bifurcation coronary lesions: the 15th consensus document from the European Bifurcation Club. *EuroIntervention.* 2021;16:1307-17.

2. Finet G, Derimay F, Motreff P, Guerin P, Pilet P, Ohayon J, Darremont O, Rioufol G. Comparative Analysis of Sequential Proximal Optimizing Technique Versus Kissing Balloon Inflation Technique in Provisional Bifurcation Stenting: Fractal Coronary Bifurcation Bench Test. *JACC Cardiovasc Interv.* 2015;8:1308-17.

3. Kassab GS, Finet G. Anatomy and function relation in the coronary tree: from bifurcations to myocardial flow and mass. *EuroIntervention.* 2015;11 Suppl V:V13-7.

4. Finet G, Gilard M, Perrenot B, Rioufol G, Motreff P, Gavit L, Prost R. Fractal geometry of arterial coronary bifurcations: a quantitative coronary angiography and intravascular ultrasound analysis. *EuroIntervention.* 2008;3:490-8.

5. Foin N, Sen S, Allegria E, Petraco R, Nijjer S, Francis DP, Di Mario C, Davies JE. Maximal expansion capacity with current DES platforms: a critical factor for stent selection in the treatment of left main bifurcations? *EuroIntervention.* 2013;8:1315-25.

6. Ng J, Foin N, Ang HY, Fam JM, Sen S, Nijjer S, Petraco R, Di Mario C, Davies J, Wong P. Over-expansion capacity and stent design model: An update with contemporary DES platforms. *Int J Cardiol.* 2016;221:171-9.

7. Ding D, Huang J, Westra J, Cohen DJ, Chen Y, Andersen BK, Holm NR, Xu B, Tu S, Wijns W. Immediate post-procedural functional assessment of percutaneous coronary intervention: current evidence and future directions. *Eur Heart J.* 2021;42:2695-707.

8. Räber L, Mintz GS, Koskinas KC, Johnson TW, Holm NR, Onuma Y, Radu MD, Joner M, Yu B, Jia H, Meneveau N, de la Torre Hernandez JM, Escaned J, Hill J, Prati F, Colombo A, di Mario C, Regar E, Capodanno D, Wijns W, Byrne RA, Guagliumi G; ESC Scientific Document Group. Clinical use of intracoronary imaging.

Part 1: guidance and optimization of coronary interventions. An expert consensus document of the European Association of Percutaneous Cardiovascular Interventions. *Eur Heart J.* 2018;39:3281-300.

9. Johnson TW, Räber L, di Mario C, Bourantas C, Jia H, Mattesini A, Gonzalo N, de la Torre Hernandez JM, Prati F, Koskinas K, Joner M, Radu MD, Erlinge D, Regar E, Kunadian V, Maehara A, Byrne RA, Capodanno D, Akasaka T, Wijns W, Mintz GS, Guagliumi G. Clinical use of intracoronary imaging. Part 2: acute coronary syndromes, ambiguous coronary angiography findings, and guiding interventional decision-making: an expert consensus document of the European Association of Percutaneous Cardiovascular Interventions. *Eur Heart J.* 2019;40:2566-84.

10. Medrano-Gracia P, Ormiston J, Webster M, Beier S, Young A, Ellis C, Wang C, Smedby Ö, Cowan B. A computational atlas of normal coronary artery anatomy. *EuroIntervention.* 2016;12:845-54.

11. Williams PD, Mamas MA, Morgan KP, El-Omar M, Clarke B, Bainbridge A, Fath-Ordoubadi F, Fraser DG. Longitudinal stent deformation: a retrospective analysis of frequency and mechanisms. *EuroIntervention.* 2012;8:267-74.

12. Ormiston JA, Webber B, Ubod B, White J, Webster MW. Stent longitudinal strength assessed using point compression: insights from a second-generation, clinically related bench test. *Circ Cardiovasc Interv.* 2014;7:62-9.

13. Ormiston JA, Webber B, Webster MW. Stent longitudinal integrity bench insights into a clinical problem. *JACC Cardiovasc Interv.* 2011;4:1310-7.

14. Sumi T, Ishii H, Tanaka A, Suzuki S, Kojima H, Iwakawa N, Aoki T, Hirayama K, Mitsuda T, Harada K, Negishi Y, Ota T, Kada K, Murohara T. Impact of post-dilatation on longitudinal stent elongation: An in vitro study. *J Cardiol.* 2018;71:464-70.

15. Matsuda Y, Ashikaga T, Sasaoka T, Hatano Y, Umemoto T, Yamamoto T, Maejima Y, Hirao K. Effectiveness of the proximal op timization technique for longitudinal stent elongation caused by post-balloon dilatation. *J Interv Cardiol.* 2018;31:624-31.

16. Gil RJ, Bil J, Kern A, Iñigo-Garcia LA, Formuszewicz R, Dobrzycki S, Vassilev D, Mehran R. Angiographic Restenosis in Coronary Bifurcations Treatment with Regular Drug Eluting Stents and Dedicated Bifurcation Drug-Eluting BiOSS Stents: Analysis Based on Randomized POLBOS I and POLBOS II Studies. *Cardiovasc Ther.* 2020;2020:6760205.

Supplementary data

Supplementary Table 1. Procedural and stent characteristics of the clinical cases.

Supplementary Figure 1. Parameters of the bench vessel models.

Supplementary Figure 2. Steps of the bench testing for the 3.00 mm stent platform (left) and for the 3.50 mm stent platform (right).

Supplementary Figure 3. Lengthening according to different stent types (A) and according to different types of stent designs (B).

Supplementary Figure 4. Lengthening in the tertiles according to extent of overdilation.

Moving image 1. Overexpansion with tight "balloon-to-strut" interaction results in longitudinal stent stretching. POT balloon, positioned with marker to carina slides backwards during opening due to "melon seed effect".

Moving image 2. Another example of longitudinal stent stretching during proximal optimisation.

The supplementary data are published online at: https://eurointervention.pcronline.com/doi/10.4244/EIJ-D-21-00824